NTHAS6: Sixth Japan-Korea Symposium on Nuclear Thermal Hydraulics and Safety
Okinawa, Japan, November 24- 27, 2008

N6P1062

# ESTIMATION OF HEAT TRANSFER COEFFICIENT AND FLOW CHARACTERISTICS ON HEAT TRANSFER TUBE IN SODIUM WATER REACTION

**Toshinori MATSUMOTO[1*], Takashi TAKATA[1], Akira YAMAGUCHI[1]**
**Akikazu KURIHARA[2], Hiroyuki OHSHIMA[2]**

*[1]Depertment of Energy and Environment Engineering, Osaka University*
*2-1 Yamada Oka, Suita, Osaka, JAPAN 565-0871*
*Tel:+81-6-6879-7895 E-mail: matsumoto_t@qe.see.eng.osaka-u.ac.jp*

*[2] Japan Atomic Energy Agency*
*4002, Narita, O-arai, Higashi-Ibaraki, Ibaraki, Japan*

## ABSTRACT

In a steam generator of FBR, a high pressured water flows inside of heat transfer tubes and exchanges its heat with sodium through the tubes. When a tube fails, water would leak into sodium, and react with sodium (Sodium Water Reaction; SWR). This reaction occurs rapidly and accompanies a high temperature jet. The jet has possibilities to cause a secondary failure of neighboring tubes. With regard to the secondary failure caused by deterioration of tube material due to high temperature (overheating rupture), quantification of heat transfer from fluid to the tube is important perspective of safety evaluation. The SWR experiments with SWAT-1R test facility was performed at Japan Atomic Energy Agency (JAEA). In the experiment, the SWR was produced by feeding water vapor from one tube toward a test section of pin bundle with 43 tubes. Thermo couples (T/Cs) were installed and temperature transient was measured in a certain tube near the reacting zone. In the present study, the heat transfer coefficient on the heat transfer tube has been investigated numerically based on the experimental temperature. Furthermore, we also have made an investigation of the flow characteristic on the heat transfer tube, taking into account the variation of the heat transfer coefficient.

## 1. INTRODUCTION

Sodium is supposed to be coolant for fast breeder reactor (FBR). In a steam generator of FBR, water flows inside of the heat transfer tubes while sodium flows in the shell side. When a tube fails, water vapor would leak into sodium and sodium water reaction (SWR) would take place. The SWR generates high temperature reacting zone which covers up surrounding tubes. Hence, the tubes have possibilities to fail secondarily because of strength deterioration caused by high temperature (so called overheating rupture).

To evaluate possibility of the secondary failure, estimating temperature of the neighbor tube is significant. Amount of heat transfer from fluid to the tube can be evaluated with a heat transfer coefficient. The heat transfer coefficient is affected by such as fluid properties and characteristics.

Statuses of the SWR such as distributions of void fraction, temperature and product of the reaction have not been known well. In order to observe a temperature distribution during the SWR, SWAT-1R experiment (Nishimura *et al.*, 2003) was run at Japan Atomic Energy Agency (JAEA). In the experiments, fluid temperatures and material temperature of the tube near the reacting zone were measured. In this paper, the heat transfer coefficient between the tube and fluid in the SWR has been analyzed numerically based on the SWAT-1R experiment. Furthermore, the flow characteristics of the measurement point have also been conjectured from the heat transfer coefficient.

## 2. SWAT-1R EXPERIMENT

Figure1 shows outline of the test section of SWAT-1R. The test section consists of 43 tubes which are mocked up the heat transfer tubes of steam generator in Japanese prototype fast breeder reactor 'Monju'. The test section was filled with stagnant liquid sodium. The outer tube diameter is 31.8 mm and the thickness is 3.8 mm. As a failed tube, one tube for water vapor injection is arranged at the bottom of the test section (see gray colored tube in Fig.1). Pressurized water vapor at 16.8MPa and 350°C flows inside of the failed tube. Water vapor was blown out vertically from the leakage that is 5.8 mm in diameter and is located at the top of the failed tube for approximately 30 seconds. A Heat transfer tube for measurement of the temperature is arranged at approximately 100mm above the leakage (hatched line tube). Temperature was measured with thermo couples (T/C) that were arranged in three axial locations as shown in the left side of Fig.1. Locations B and E are placed just above the water vapor leakage nozzle. Locations A, D and C, F are located in 50mm away from Locations B and E in the axial direction.

Figure 2 shows a detail of temperature measurement. One T/C is arranged in the liquid sodium side at 2mm from the tube surface (Point a). Another two T/Cs are embedded inside the tube wall (Point b and c). In each point, temperature time history in the fluid and the tube wall were measured during the experiment.

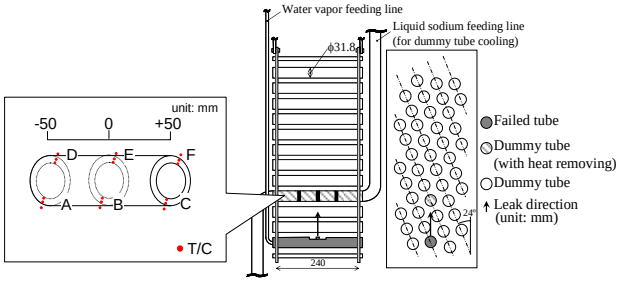


**Fig.1 Outline of SWAT-1R**

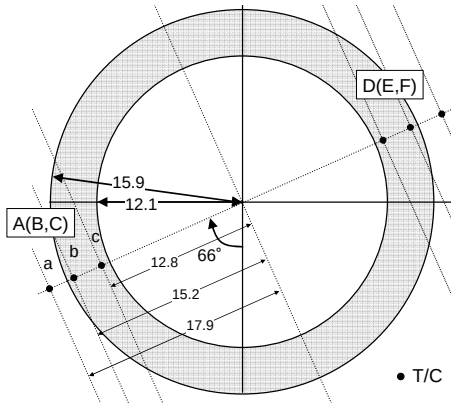


**Fig.2 Location of T/Cs**

## 3. NUMERICAL METHOD

Temperature of the heat transfer tube is computed by solving one dimensional heat transfer conduction equation in cylindrical coordinate. The governing equation is described as:

$$\rho C_p \frac{\partial T}{\partial t} = \frac{1}{r}\frac{\partial}{\partial r}\left( r\lambda \frac{\partial T}{\partial r} \right) \quad (1)$$

where $\lambda$, $\rho$ and $C_p$ are the thermal conductivity, the density and the specific heat respectively. $T$, $r$ and $t$ are the temperature and the radial coordinate and the time respectively.
Equation (1) is discretized based on a control volume of each computational cell as:

$$\rho C_p \frac{T_i - T_i^0}{\Delta t}\Delta V = -\lambda_{i-1/2}\frac{T_i - T_{i-1}}{r_i - r_{i-1}}A_{i-1/2} + \lambda_{i+1/2}\frac{T_{i+1} - T_i}{r_{i+1} - r_i}A_{i+1/2} \quad (2)$$

where subscript $i$ indicates the i-th control volume. Superscript 0 means the temperature in the last time step. $\Delta t$ is the time step. $A$ is cross sectional area at the boundary of the control volume. $\Delta V$ is the volume of the computational cell. Subscript $i\pm1/2$ means the boundary between control volumes.

At the outer surface of the tube, a heat transfer coefficient is introduced to evaluate a heat flux between the heat transfer tube and the adjoining fluid. Schematic of the outer surface is shown in Fig.3. At the outermost computational cell, the governing equation of energy is descretized in the following:

$$\rho C_p \frac{T_{i\max} - T_{i\max}^0}{\Delta t}\Delta V = -\lambda_{i-1/2}\frac{T_{i\max} - T_{i\max-1}}{r_{i\max} - r_{i\max-1}}A_{i\max-1/2} + \frac{T_f - T_i}{\frac{r_b - r_i}{\lambda_i} + \frac{1}{h}}A_{i+1/2} \quad (3)$$

where $h$ is heat transfer coefficient. $T_f$ is temperature of fluid.

To closure Eqs. (2) and (3), one has to obtain the value of the heat transfer coefficient. On the other hand, two tube temperatures (Points b and c) and the fluid temperature (Point a) were measured at each radial direction in the experiment (see Fig.2). Therefore, we have evaluated the heat transfer coefficient by solving the inverse problem of Eqs. (2) and (3) in the following manner.

As a boundary condition, the inner temperature of the tube (point c) and the fluid temperature (point a) are determined from the experimental results. At the beginning of each computational time step, a certain heat transfer coefficient is assumed and Eqs. (2) and (3) are solved using the Tri Diagonal Matrix Algorithm (TDMA). Then, a bi-section method is applied, by changing the heat transfer coefficient and solving Eqs. (2) and (3) iteratively, so that the temperature at Point b coincides with the experimental result in a convergence criterion.

It is noted that no solution of the heat transfer coefficient is obtained sometimes during the computation. At that time, the actual time is incremented by the time step until one achieves the solution of Eqs. (2) and (3). As a result, an average heat transfer coefficient during several time steps is evaluated at that situation.

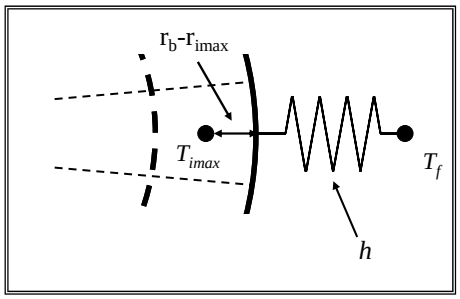


**Fig.3 Heat transfer coefficient at surface of the tube**

## 4. NUMERICAL INVESTIGATION OF HEAT TRANSFER COEFFICIENT IN SWAT-1R EXPERIMENT

### 4.1 Numerical Conditions

In the computation, time step is set to 0.05 seconds which is same as the measurement interval in the experiment. The temperature measurement was carried out from 5 seconds before the water injection to 30 seconds after the finish of the injection (65 seconds in total). Hence the same time duration is applied in the analysis.

As concerns the convergence criterion of the bi-section method, $1.0\times10^{-10}$ °C is applied in the present study.

In the numerical investigation, physical properties of the tube material (2-1/4Cr-1Mo) are defined with the following correlations (Takasu *et al.*, 1981) as:

$$C_p = (0.38011\times10^{-7}\times T_F + 0.19226\times10^{-4})\times T_F + 0.105543\ (\text{kcal/kg/}^\circ\text{F}) \quad (4)$$

$$\rho = 2.768\times10^4\{(-0.177497\times10^{-8}\times T_F - 0.468057\times10^{-5})\times T_F + 0.282350\}\ (\text{kg/m}^3) \quad (5)$$

$$\alpha = \exp\{(-0.16954\times10^{-6}\times T_F - 0.24785\times10^{-3})\times T_F - 0.844030\}\frac{1}{10.76}\ (\text{m}^2/\text{h}) \quad (6)$$

where $T_F$ means temperature degrees Fahrenheit and, $\alpha$ is the thermal diffusivity. The thermal conductivity is calculated by multiplying specific heat, density and thermal diffusivity.

Figures 4, 5 and 6 show the temperature dependency of the properties. Physical properties measured in a material test (Kimura *et al.*, 1990) are also indicated as a reference. Material properties obtained with the correlations do not agree with the measurement especially in high temperature region. Specific heat obtained the measurement increases suddenly around 765 °C and 815 °C. This increase was caused by phase transition such as the magnetic phase transition and the structural transition (Kimura *et al.*, 1990). It may be said that the present correlations (Eqs. 4 to 6) has a little bit low accuracy in high temperature region that has been observed in the SWR phenomena.

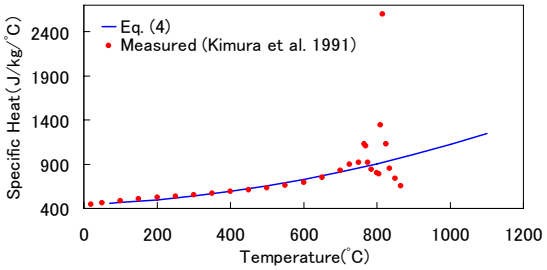


**Fig. 4 Specific Heat**

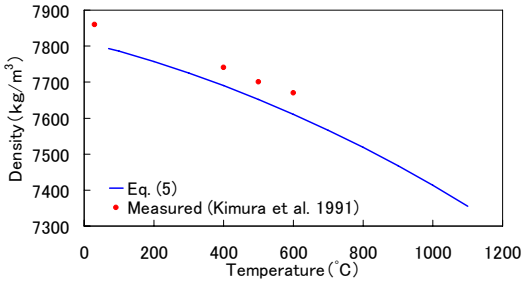


**Fig. 5 Density**

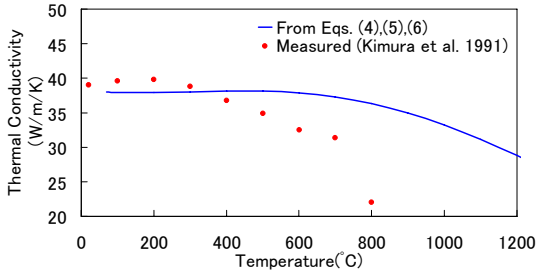


**Fig. 6 Thermal Conductivity**

### 4.2 Results and Discussions

When the SWR takes place, the reacting gas will collide with the bottom side of the heat transfer tube (Locations A, B and C). So the bottom side is discussed firstly. It is noted that the heat transfer coefficient of Location B has not been evaluated because the impractical temperature was measured at Point a of Location B during the experiment.

According to a previous work (Yamaguchi et al., 2007), the heat transfer coefficient has been evaluated to 12,000 W/m$^2$/K by one-dimensional thermal-hydraulics simulation based on a boundary layer approximation in which the void fraction of 0.94 has been assumed.

It is also noted that, the heat transfer coefficient is evaluated approximately 30,000 W/m$^2$/K on the assumption that stagnant liquid sodium fill between the surface of the tube and Point a and that the thermal conductivity is only considered.

#### *4.2.1 Bottom side (Location A and C)*

Figures 7 and 8 show the computed heat transfer coefficient and the temperature trend of the fluid side (Point a) at Location A and C, respectively. Table 1 shows the time weighted average and the median value of the heat transfer coefficient at a typical period that is roughly divided by its behavior.

**Table 1 Representative value of heat transfer coefficients at Locations A, B and C**

| Location | Time (s) | Heat Transfer Coefficient (W/m$^2$/K) | |
|---|---|---|---|
| | | Time Average | Median value |
| A | 0.0-2.0 | 28,071 | 34,181 |
| | 2.0-5.0 | 26,340 | 26,452 |
| | 5.0-18.0 | 145,328 | 42,650 |
| | 18.0-30.0 | 218,129 | 112,641 |
| B | - | - | - |
| C | 0.0-8.0 | 14,897 | 14,940 |
| | 8.0-17.0 | 27,486 | 25,413 |
| | 17.0-30.0 | 861,058 | 128,335 |

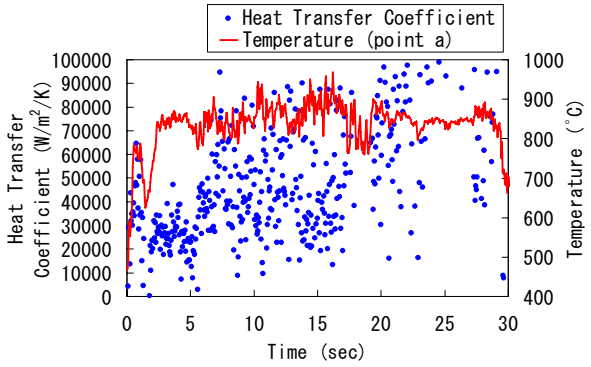


**Fig. 7 Heat Transfer Coefficient (A)**

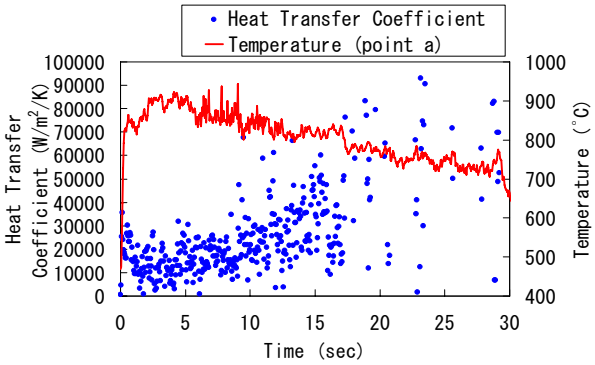


**Fig. 8 Heat Transfer Coefficient (B)**

During the first 2 seconds at Location A, the instantaneous heat transfer coefficient, shown in Fig.7, seems to be a fair bit high (approximately 40,000 to 60,000 W/m$^2$/K) comparing with the previous work (=12,000 W/m$^2$/K) in the very beginning of the experiment. At the same time, the representative heat transfer coefficient is approximately 30,000 W/m$^2$/K both in the time weighted average and the median as in Table 1. In the previous work, the high void fraction (0.94) was assumed and the heat transfer coefficient will increase as the void fraction decreases. Accordingly, it can be said that the gas region due to the SWR develops and covers gradually over Location A in this period.

From 2 to 5 seconds, the variation of the coefficient and the liquid sodium temperature seems to be decreased as seen in Fig.7. The time average and the median of the coefficient are almost the same (approximately 26,000 W/m$^2$/K). It is expected that a quasi-steady state of reacting zone where the void fraction is a little bit lower than 0.94 appears at Location A.

From 5 seconds to 18 seconds, the heat transfer coefficient increase to 140,000 W/m$^2$/K in the time average and 40,000W/m$^2$/K in the median. Due to the appearance of some extraordinary large values in the computed heat transfer coefficient, these two values largely differed. To clarify the difference between the time weighted average and the median, the temperature at Point b has been compared numerically. In this analysis, the temperature history at Points a and c are used for boundary condition and, the representative values (Table 1) are applied.

The comparison of the temperature history at the Point b is shown in Fig.9. The temperature history measured in the experiment and the results of the computation with the constant heat transfer coefficient (obtained in the previous work, 12,000 W/m$^2$/K) are also indicated in Fig.9. The result using the median value follows the measured history well. Hence the median value is used for investigation of the following results.

In case of the constant heat transfer coefficient, the temperature history is evaluated lower than the experiment. Again it can be said that the gas fraction is lower than the 0.94 as presumed in the previous work.

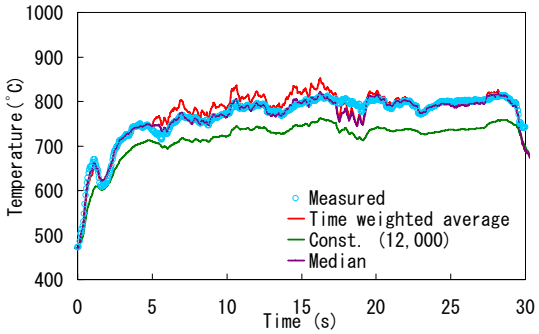


**Fig. 9 Temperature history (A)**

After 18 seconds, the heat transfer coefficient is estimated over 100,000 W/m$^2$/K. Therefore the influence of the liquid phase is presumed extremely high. Let us investigate a validity of the heat transfer coefficient (the median value 113,000W/m$^2$/K) simply. Here it is assumed that the measurement location was covered up fully by liquid sodium. The following correlation (Subbotin equation (7) (JSME, 1986)) is used to estimate the liquid velocity in which the tube diameter is defined as a characteristic length.

$$Nu = 5 + 0.025 Pe^{0.8} \tag{7}$$

here, $Nu$ and $Pe$ means the Nusselt number and the Peclet number respectively. $Nu$ and $Pe$ can be written as:

$$Nu = hL/\lambda \tag{8}$$

$$Pe = PrRe = \nu/\alpha \times UD/\nu \tag{9}$$

where $L$ means the characteristic length. $Pr$ and $Re$ means the Prandtl number and the Reynolds number. $\nu$ and $U$ is dynamic coefficient of viscosity and velocity of the fluid respectively. From Eqs. (7) to (9) the velocity is calculated as follows:

$$U = \frac{\nu}{D\,\mathrm{Pr}}\left(\frac{hL/\lambda - 5}{0.025}\right)^{1.25} \tag{10}$$

the physical properties of liquid sodium at 1,100K and 113,000W/m$^2$/K of the heat transfer coefficient is used in Eq. (10), the liquid sodium velocity is estimated to 31.1 m/s. This value seems to be practical as a local liquid velocity close to the reacting zone in the SWR phenomenon.

As in case of Location C, the high heat transfer coefficient is not evaluated instantaneously at the beginning of the SWR as seen in Fig.8. It might be concluded that the reacting zone was covered up at Location C faster than Location A. Since the representative heat transfer coefficient at Location C is lower than that at Location A during approximately 17 seconds from the beginning (median in Table 1), the gas region due to the SWR was more influential at Location C.

After 17 seconds, it is supposed that the fluid mainly consists of liquid phase, because the representative heat transfer coefficient is evaluated approximately 120,000 W/m$^2$/K. However, it is carefully noted that the temperature at Point a decreased suddenly at 17 seconds and that less computational results are obtained at that period as in Fig.8. This is attributed the fact that the temperature at Point a became close to that at Point b after 17 seconds. It may also have a possibility of T/C trouble at Location A after 17 seconds.

In case of the constant heat transfer coefficient (12,000 W/m$^2$/K), temperature at Point b is underestimated than the experiment after 10seconds from the leakage (Fig.10). This corresponds to the differences of the coefficient as shown in Table 1 (for example, the heat transfer coefficient of the median value from 8 to 17 seconds is approximately twice as high as the previous work).

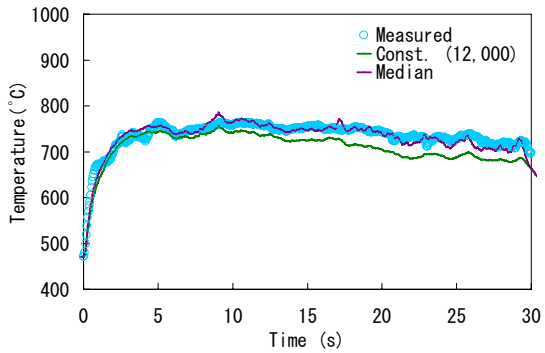


**Fig. 10 Temperature history (B)**

At the bottom side (Locations A and C) which faces to the water vapor leakage, it is concluded that the heat transfer coefficient is evaluated to 15,000 to 40,000 W/m$^2$/K during the first 18 seconds. Comparing the present result with the previous work (12,000 W/m$^2$/K) in which the void fraction was assumed to be 0.94, higher heat transfer coefficient is investigated. However, it can be said the gas region still affects dominantly at Locations A and C taking into account the thermal conductivity of stagnant liquid sodium. The heat transfer coefficient at Location A tends to be overestimated rather than that at Location C. Therefore, the influence of the gas phase may be higher at Location C and thus the reacting zone may not spread symmetrically.

After 18 seconds, the heat transfer coefficient is evaluated more than 100,000 W/m$^2$/K both at Locations A and C. Consequently, it can be said that the liquid phase affects mainly. At this period, the reacting zone will exists between Location A and C. It is noted that the T/C at Point b might have some trouble at Location C from the computational investigation.

*4.2.2 Top side of the tube (Location D, E and F)*

The computed heat transfer coefficient is shown Figs.11, 12 and 13. And the representative value of heat transfer coefficient is summarized in Table 2.

**Table 2 Representative value of heat transfer coefficient at Locations D, E and F**

| Location | Time (s) | Heat Transfer Coefficient ($W/m^2/K$) | |
|---|---|---|---|
| | | Time Average | Median value |
| D | 0-3.5 | 79,901 | 58,199 |
| | 3.5-30 | 21,687 | 19,676 |
| E | 0-5.0 | 218,752 | 50,617 |
| | 5.0-30.0 | 37,154 | 17,197 |
| F | 0-3.0 | 73,663 | 45,678 |
| | 3.0-30 | 19,650 | 16,003 |

At all locations, during the first several seconds, a comparative high heat transfer coefficient which is similar to that at Location A is investigated as shown in Figs.11 to 13 and Table 2. Again, it can be concluded that liquid sodium was swept out and that the gas region covered over the measuring location at this period. Hence the heat transfer coefficient increases temporarily caused by the flowage of the stagnant liquid sodium around the tube.

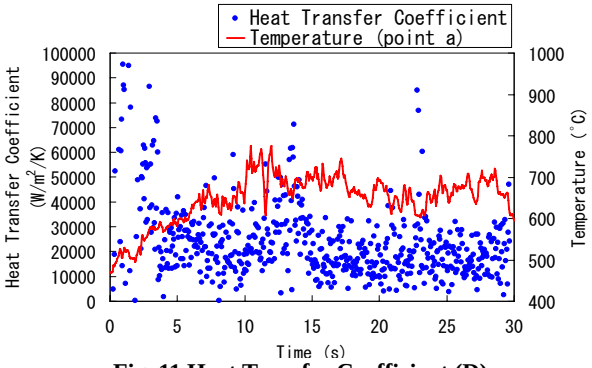


**Fig. 11 Heat Transfer Coefficient (D)**

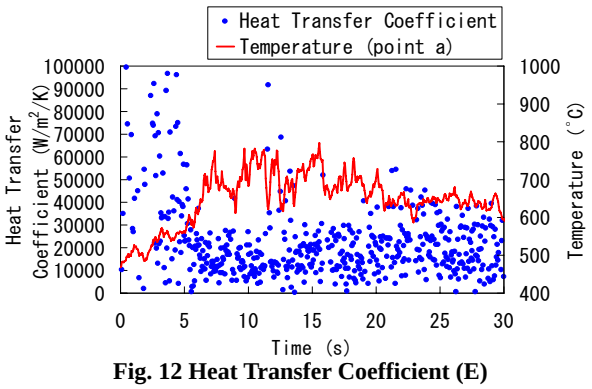


**Fig. 12 Heat Transfer Coefficient (E)**

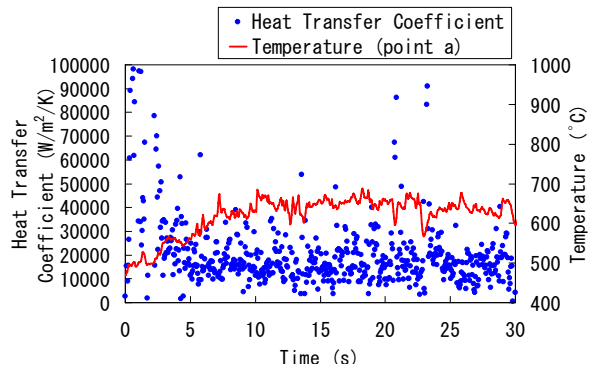


**Fig. 13 Heat Transfer Coefficient (F)**

After 5 seconds, the heat transfer coefficient is evaluated to less than 20,000 $W/m^2/K$ and is close to the previous work (12,000 $W/m^2/K$). Therefore, it is indicated that the influence of the gas phase is quite high.

In Figs.14 to 16 shows the temperature history of Point b obtained in the experiment, computed with the representative value of the heat transfer coefficient (median in Table 2) and the constant value (12,000 $W/m^2/K$). As shown in Figs.14 to 16, a good agreement is achieved both in the representative and constant values. The temperature at Position b tends to be underestimated slightly in case of the previous work (constant value) because of the underestimation of the coefficient in the beginning of the experiment (see Table 2).

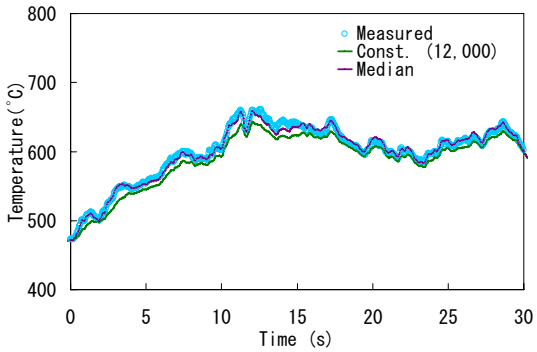


**Fig. 14 Temperature history (D)**

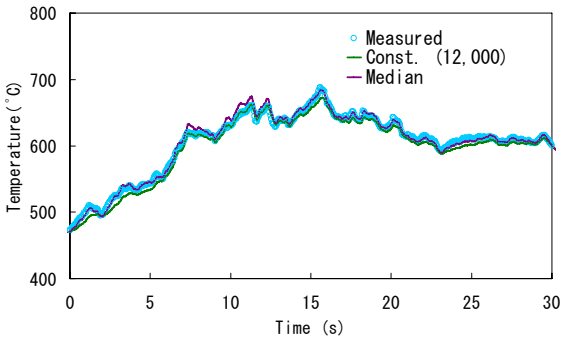


**Fig. 15 Temperature history (E)**

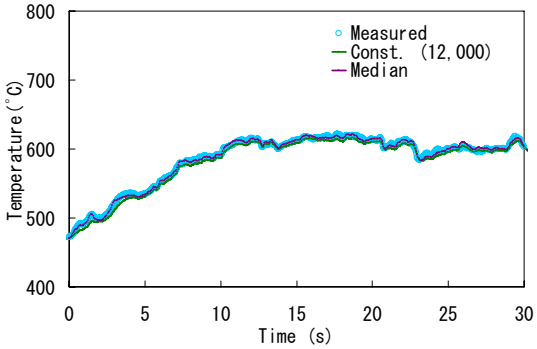


**Fig. 16 Temperature history (F)**

At Locations D, E and F, it is supposed that the gas phase has a strong influence comparing with the bottom side (Locations A and C). When the gas region collides with the heat transfer tube, it will be spread widely due to the obstacle. As a result, an extensive gas region appears at the opposite side from the leakage. Thus the lower, but close to the previous work, heat transfer coefficient is investigated at the top side regardless of the measurement location. Comparing at Location F (opposite side from Location C), the heat transfer coefficient at Location D (opposite side from Location A) seems to be a little bit higher as in Table 2. The influence of liquid phase seems to be

larger at Location A than at Location C as mentioned in sec.4.2.1. It may be said that the influence of liquid phase continues to the opposite side (Location D).

## 5. CONCLUSIONS

Numerical investigation of heat transfer coefficient from fluid to the heat transfer tube in the SWR has been carried out using the temperature data measured in the SWAT-1R experiment. One dimensional heat transfer conduction is assumed considering the heat transfer coefficient between the fluid and the tube surface. An inverse problem approach is applied to investigate the heat transfer coefficient using the measurement temperature history and a bi-section method is used to calculate the coefficient. As a representative heat transfer coefficient at a certain period, two kinds of approach (time weighted average and median value) is tested. In the present work, the median value is adopted as the represesntative value in terms of the reproducibility of the measurement temperature.

As a result of the numerical investigation of the heat transfer coefficient in the SWAT-1R experiment, it is demonstrated that the higher heat transfer coefficient is estimated at the bottom side of the heat transfer tube which faces to the leakage during first 18 seconds from the leakage, comparing with the previous work.

However, it can be said the gas region affects dominantly at that period when one takes into account the conductive heat transfer by stagnant liquid sodium. Probably, the void fraction may be a little bit lower than the previous work (0.94).

After 18 seconds, considerably high heat transfer coefficient is predicted at the bottom side (more than 100,000 $W/m^2/K$). It will be concluded that the liquid phase is dominant in this period and that the reacting zone exists between the measurement locations (Locations A and C). It is also mentioned that the trend and magnitude of the heat transfer coefficient differs from each location, which is arranged symmetrically from the leakage. Thus the reacting zone would be developed asymmetrically.

At the top side of the tube, the similar value of the heat transfer coefficient with the previous work is predicted regardless the locations during the SWR, although several times higher value is investigated at first several seconds. In the beginning of the SWR, the heat transfer coefficient would increase temporarily caused by the flowage of the stagnant liquid sodium around the tube.

When the reacting zone (gas region) collides with the heat transfer tube, it will be spread widely due to the obstacle. Hence an extensive gas region appears at the opposite side from the leakage resulting in the present investigation.

In the future work, to practice advanced numerical analysis, in addition to evaluation of temperature history, evaluation heat transfer from fluid to the tube by estimation of flow field based on boundary layer approximation is being planed. Furthermore, the quantification of the secondary failure of overheating rupture is also being planned.

## NOMENCLATURE

| | | |
|---|---|---|
| $A$ | cross sectional area | $[m^2]$ |
| $C_p$ | specific heat | $[J/kg/°C]$ |
| $h$ | heat transfer coefficient | $[W/m^2/K]$ |
| $L$ | characteristic length | [m] |
| $Nu$ | Nusselt number | |
| $Pe$ | Peclet number | |
| $Pr$ | Prandtl number | |
| $Re$ | Reynolds number | |
| $r$ | radial coordinate | [m] |
| $T$ | temperature | [°C] |
| $T_f$ | temperature of fluid | [°C] |
| $T_F$ | temperature degrees Fahrenheit | [°F] |
| $t$ | time | [s] |
| $U$ | velocity of the fluid | [m/s] |

**Greek Letters**

| | | |
|---|---|---|
| $\alpha$ | thermal diffusivity | $[m^2/s]$ |
| $\Delta t$ | time step | [s] |
| $\Delta V$ | volume of the cell | $[m^3]$ |
| $\lambda$ | thermal conductivity | [W/m/K] |
| $\nu$ | dynamic coefficient of viscosity | $[m^2/s]$ |
| $\rho$ | density | $[kg/m^3]$ |

**Subscripts/Superscripts**

| | |
|---|---|
| $i$ | i-th control volume |
| $i\pm1/2$ | boundary between control volumes |
| $0$ | temperature in the last time step |

## REFFERENCES


JSME (1986). “JSME Data Book: Data Book 4th Edition” *JSME*

Kimura, H et al. (1990). “Measurement of Physical properties of FBR structural materials -<part1> Measurement of Physical properties of the rolled steels –” *PNC technical paper* TN9410, 90-094

Nishimura, M et al. (2003). “Sodium-Water reaction test to confirm thermal influence on heat transfer tubes” *JNC technical paper* TN9400, 2003-014

Takasu, H et al. (1981). “Physical Properties for Sodium Technology (Na, Ar, He, 304SS, 316SS, 21/4Cr-1Mo)” *PNC technical paper* PNC N941 81-73